Synthesis of Tb^{3+}-doped ZnO Nanowire Arrays Through a Facile Sol–Gel Template Approach

Lei Yang,* Yan Li, Yanhe Xiao, Changhui Ye, and Lide Zhang
Key Laboratory of Material Physics, Institute of Solid State Physics, Chinese Academy of Sciences, P. O. Box 1129, Hefei 230031, P. R. China

(Received March 3, 2005; CL-050288)

Ordered Tb^{3+}-doped zinc oxide nanowire arrays embedded in anodic alumina membranes (AAM) were fabricated by an improved sol–gel method. They have hexagonal wurtzite structure with uniform diameter of about 30 nm and the Tb^{3+} ions occupy Zn sites or interstitial sites in the crystal. The emission spectra of ZnO:Tb consist of four main lines at 488 nm, 543 nm, 586 nm, and 622 nm under 377 nm excitation, among which the electric dipole transition $^5D_4 \rightarrow {}^7F_5$ (at 543 nm) is the strongest.

Since the discovery of carbon nanotubes, there have been many reports on the synthesis of one-dimensional nanomaterials, such as nanorods, nanobelts, nanotubes, and nanocables.[1–5] ZnO, with direct bandgap of 3.37 eV at room temperature, is recognized as a promising photonic material for optoelectronic devices, field-emission displays, and gas sensors.[6–9] In particular, ZnO is regard as a promising candidate material for flat panel displays because of its high electrical conductivity, high optical transparency as well as its low cost and easy etchability. If rare earth (RE) ions are incorporated into ZnO, optical properties of which are expected to be modified remarkably. For example, ZnO doped with Eu can emit red light and ZnO doped with Er or Tb can emit green light.[10–12] Among the rare earth elements, luminescence of Tb^{3+} is particularly interesting because the major emission band is centered near 544 nm, which is one of the three primary colors. However, it is difficult to incorporate RE ions effectively into ZnO nanocrystals using chemical vapor deposition (CVD) method or the electrochemical deposition method because of the high melting point of ZnO and RE_2O_3 and high standard electrode potential of RE. In this study, Tb^{3+}-doped ZnO nanowire arrays were prepared successfully by an improved sol–gel method using porous anodic alumina membranes (AAM).[13] To the best of our knowledge, no reports on the synthesis of Tb^{3+}-doped zinc oxide nanowire arrays embedded in AAM have been published to date.

AAM used in this work is formed via anodization of aluminum metal in 0.3 M oxalic acidic solution, which has been studied in detail over the last five decades.[14] Nitrate of Tb was prepared by dissolving terbium oxide in nitric acid, and addition of several drops of H_2O_2 is necessary in the dissolving process. Ethylene glycol and urea used in this experiment were A.R. grade. In this experiment, 0.3 g of $Zn(NO_3)_2 \cdot 6H_2O$ was dissolved into 100 mL of deionized water to form a 0.01 M aqueous solution. Nitrate of Tb was added into the solution. The molar ratio of Tb to Zn was 2.5, 5, 7.5, 10, and 12.5% each. The pH value of the solution was adjusted to near neutral using aqueous amonia and dilute nitric acid. Then 0.3 g of urea and 5 mL of ethylene glycol were added into the solution. The AAM was placed in a beaker that contained the above-mentioned mixed solution and then the beaker was sealed with adhesive tape. Subsequently, the beaker was kept at 60 °C for 48 h and then at 80 °C for 48 h. Finally, the AAM was taken out to wash repeatedly and then placed in the muffle furnace which was kept at 700 °C for 10 h. The sample must be treated by 5 wt % NaOH before it was observed by TEM.

The as-synthesized sample was examined by X-ray diffraction (XRD) measurements on a Philips X'pert PRO diffractometer (Cu Kα). The morphology of the as-synthesized sample was obtained with transmission electron microscopy (TEM JEM-2021) and scanning electron microscopy (FE-SEM Sirion 200). X-ray photoemission spectroscopy (XPS) measurement were carried out with a monochromatic Al Kα radiation source on a VG ESCALAB Mark II X-ray photoemission spectrometer. Room temperature photoluminescence was recorded with an Edinburgh luminescence spectrometer (FLS 920) using a xenon lamp as the excitation source.

Five XRD patterns of the as-prepared samples doped with the molar ratio of Tb to Zn of 2.5, 5, 7.5, 10, and 12.5%, respectively, are shown in Figure 1. The diffraction peaks can be indexed to a hexagonal wurtzite structure of ZnO. Compared with JCPDS data, all the diffraction peaks are shifted slightly towards the low diffraction angle indicating that the lattice parameters of Tb-doped ZnO are a little larger than those of undoped ZnO. No XRD peaks related to Tb compounds were found. So it is believed that Tb^{3+} ions occupy Zn sites or interstitial sites in ZnO lattice.

The morphology of the as-synthesized sample was obtained with FE-SEM and TEM. Figure 2a displays the top view SEM image of the ZnO:Tb nanowire arrays grown within an AAM. The transmission electron microscopy images of the product are shown in the Figure 2b. The image of a single ZnO:Tb nanowire is shown in Figure 2c. The inset of Figure 2c presents the selected area electron diffraction (SAED) pattern taken from the single nanowire. It can be observed that large-scale polycrystals were produced with the uniform about 30 nm. The micrograph shows that the ZnO:Tb nanowires are roughly parallel to each other, and vertically to the AMM surface. It is found that almost all the pores in AMM are filled with ZnO:Tb nanowire.

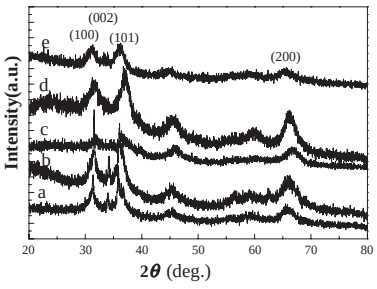

Figure 1. XRD diffraction patterns of ZnO:Tb nanowire arrays. The molar ratio of Tb to Zn: a 2.5%, b 5%, c 7.5%, d 10%, e 12.5%.

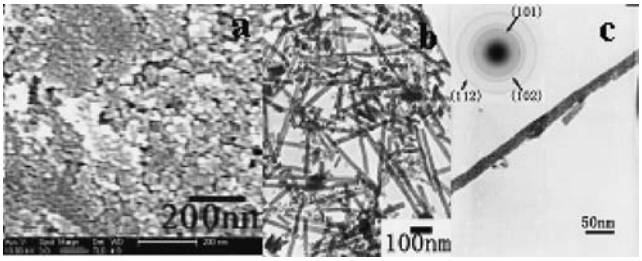

Figure 2. The SEM and TEM images of ZnO:Tb nanowire arrays. (a) typical SEM image of ZnO:Tb nanowire arrays, (b) typical TEM image of the ZnO:Tb nanowires, (c) TEM image of a single ZnO:Tb nanowire and its selected area electron diffraction pattern (insert).

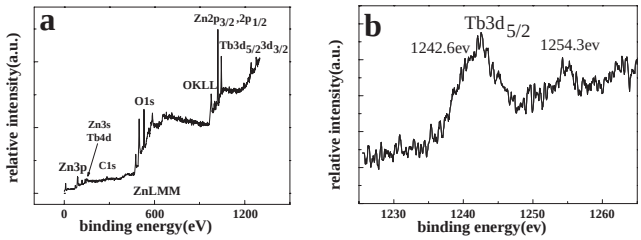

Figure 3. (a) XPS of the sample doped with the molar ratio of Tb to Zn = 10%. (b) $Tb3d_{5/2}$ core level X-ray photoelectron spectra of ZnO:Tb nanowires arrays.

Further evidence for the composition was obtained by the XPS. Figure 3a is survey spectrum and Figure 3b shows XPS spectrum taken from the $Tb3d_{5/2}$ regions of the ZnO:Tb nanowires array. In Figure 3a, there are two peaks at about 1242 and 1277 eV, which are attributed to photoemission peaks from $Tb3d_{5/2}$ and $Tb3d_{3/2}$. $Zn2p_{3/2}$, $Zn2p_{1/2}$ and O1s are also found. The atomic composition of Tb, Zn, and O was calculated by using the integrated peak area and sensitivity factors, and the atomic ratio of Tb:Zn:O is about 0.1:1:1. In the Figure 3b there are two peaks at 1242.6 and 1254.3 eV, which are attributed to photoemission peaks from $Tb3d_{5/2}$ and energy loss structure, respectively. Compared with standard peak of $Tb3d_{5/2}$ (1241.2 eV) in the Tb_2O_3, there are a blue-shift in the spectrum indicating that the distance of Tb to O in the ZnO:Tb crystal is different from the distance of Tb to O in the Tb_2O_3 oxide. It indicates that Tb^{3+} ions occupy the Zn sites or interstitial sites in ZnO lattice.

A schematic of the possible formation process of ZnO:Tb is proposed.[14] The OH^- from hydrolyzed urea combined with Zn^{2+} and Tb^{3+} to form sol when the solution was heated at above 60 °C. Sol particles can enter into the pores of AMM uninterruptedly because sol particles were negatively charged particles and the pore walls of AMM were positively charged. The sol within the AMM would be changed into gel and then turn into nanocrystallines during the sintering process.

The luminescence spectra of 5 samples at room temperature are shown in Figure 4. Figure 4a shows the excitation spectra and Figure 4b shows the emission spectra. Each excitation spectrum monitored at 544 nm for the ZnO:Tb has four peaks at 349 nm, 368 nm, 375 nm, and 487nm, respectively. All peaks represent electronic transitions in 4f energy levels of Tb^{3+}.[15] Electronic transition of $^7F_6 \rightarrow {}^5G_6$ (375 nm) is the strongest excitation peak and $^7F_6 \rightarrow {}^5D_4$ (487 nm) is very weak.[16] It indicates that

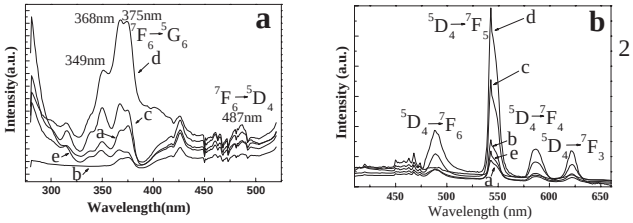

Figure 4. (a) The excited spectra of ZnO:Tb nanowire arrays. The molar ratio of Tb to Zn: a 2.5%, b 5%, c 7.5%, d 10%, and e 12.5%, (b) The emission spectra of ZnO:Tb nanowire arrays. The molar ratio of Tb to Zn: a 2.5%, b 5%, c 7.5%, d 10%, and e 12.5%.

these is an effective energy transmission from $^5G_6$ to $^5D_4$. The emission spectra for ZnO:Tb consist of four main lines at 488 nm ($^5D_4 \rightarrow {}^7F_6$), 543 nm ($^5D_4 \rightarrow {}^7F_5$), 586 nm ($^5D_4 \rightarrow {}^7F_4$), and 622 nm ($^5D_4 \rightarrow {}^7F_3$) under 377 nm excitation, which correspond to electric dipole transitions of the Tb^{3+} ions, and the electronic transition,$^5D_4 \rightarrow {}^7F_5$, is the strongest.[17,18] No luminescence of ZnO was found. From Figure 4b, it can be seen that the peak of ZnO doped with 10% of Tb^{3+} is highest and ZnO doped with 12.5% of Tb^{3+} is weak.

In summary, ordered Tb^{3+}-doped zinc oxide nanowire arrays embedded in AAM were prepared successfully by an improved sol–gel method. The nanowires with the uniform diameter of about 30 nm have hexagonal wurtzite structure and lattice parameters of Tb-doped ZnO are a little larger than those of undoped ZnO. The emission spectra for ZnO:Tb consist of four main lines, and the electric dipole transition,$^5D_4 \rightarrow {}^7F_5$, is the strongest.

This work was supported by the Ministry of Science and Technology of China (Grant No. 1999064501).

References

1 N. P. Balsara and S. Ijima, *Nature*, **354**, 54 (1991).
2 Z. W. Pan, Z. R. Dai, and Z. L. Wang, *Science*, **291**, 1947 (2001).
3 L. D. Zhang, G. W. Meng, and F. Phillipp, *Mater. Sci. Eng., A*, **286**, 34 (2000).
4 G. S. Chen, S. H. Chen, X. G. Zhu, Y. O. Mao, and L. D. Zhang, *Mater. Sci. Eng., A*, **286**, 165 (2000).
5 D. W. Wang, A. J. Millis, and S. D. Sarma, *Phys. Rev. Lett.*, **85**, 85 (2000).
6 B. C. Cheng, Y. H. Xiao, G. S. Wu, and L. D. Zhang, *Appl. Phys. Lett.*, **84**, 416 (2004).
7 Y. F. Lu, H. Q. Ni, Z. H. Mai, and Z. M. Ren, *J. Appl. Phys.*, **88**, 498 (2000).
8 N. Jayadev Dayan, S. R. Sainkar, R. N. Karekar, and R. C. Aiyer, *Thin Solid Films*, **325**, 254 (1998).
9 J. Zhong, A. H. Kitai, P. Mascher, and W. Puff, *J. Electrochem. Soc.*, **140**, 3644 (1993).
10 Y.-K. Park, J.-I. Han, and M.-G. Kwak, *Appl. Phys. Lett.*, **72**, 668 (1998).
11 M. Kohls, M. Bonanni, L. Spanhel, D. Su, and M. Giersig, *Appl. Phys. Lett.*, **81**, 3858 (2002).
12 S. M. Liu, F. Q. Liu, H. Q. Guo, Z. H. Zhang, and Z. G. Wang, *Phys. Lett. A*, **271**, 128 (2000).
13 G. S. Wu, L. D. Zhang, B. C. Cheng, T. Xie, and X. Y. Yuan, *J. Am. Chem. Soc.*, **126**, 5976 (2004).
14 R. Boyn, *Phys. Status Solidi B*, **148**, 11 (1988).
15 F. Keller, M. S. Hunter, and D. L. Robinson, *J. Electrochem. Soc.*, **100**, 411 (1953).
16 D. Ananias, A. Ferreira, J. Rocha, P. Ferreira, P. Rainho, C. Morais, and L. D. Carlos, *J. Am. Chem. Soc.*, **123**, 5735 (2001).
17 J. G. Reifenberger, G. E. Snyder, G. Baym, and P. R. Selvin, *J. Phys. Chem. B*, **107**, 12862 (2003).
18 G. Jones, II and I. Valentine, *Photochem. Photobiol. Sci.*, **1**, 925 (2002).

Published on the web (Advance View) May 21, 2005; DOI 10.1246/cl.2005.828